

Received April 17, 2020, accepted April 29, 2020, date of publication May 19, 2020, date of current version November 2, 2020.

Digital Object Identifier 10.1109/ACCESS.2020.2995744

# Open-Closed-Loop Iterative Learning Control With a Self-Adjustive Factor of the Gas Tungsten Arc Welding (GTAW) Process

NAN YIN<sup>1</sup>, LIU HANWEN<sup>2</sup>, AND YANG WU<sup>3</sup>

<sup>1</sup>Business School, Nanjing Xiaozhuang University, Nanjing 211171, China

<sup>2</sup>Department of Transportation Engineering, Tongji University, Shanghai 200092, China

<sup>3</sup>School of Electronic Engineering, Wuxi Taihu University, Wuxi 214068, China


Corresponding author: Nan Yin (kitupfor@163.com)

**ABSTRACT** Human welder's experiences and skills are critical for producing quality welds in manual gas tungsten arc welding (GTAW) process. For batch welding of the same workpiece, and the welding experience accumulated in same welding track, the welding process has a very high-degree reduplication. In this article, an open-closed-loop iterative learning control algorithm is constructed and implemented as an intelligent controller in automated GTAW process to reach the desired trajectory well. During the welding process, there will encounter external interference, such as random changes in voltage, resulting in pool surface fluctuations. Therefore, we introduce a self-adjustive factor based on ILC algorithm. The self-adjustive factor can adjust the input of the controller according to the error and error rate of change of the system, so that the system body has self-adaptation to improve the ability of anti-interference of the system. The simulation shows that a new proposed ILC control is an effective method for weld penetration in GTAW.

**INDEX TERMS** Gas tungsten arc welding, self-adjustive factor, open-closed-loop, iterative learning control.

## I. INTRODUCTION

Manual gas tungsten arc welding (GTAW) process [1]–[4], which is a reliable efficient and practical metal filling process, is commonly used in industry especially in the applications requiring high weld quality (such as aerospace, automobile, transportation and petroleum, etc.). During this process human welders can appraise the state of weld joint penetration through their observation on the weld pool and intelligently adjust the welding parameters [5]–[7] accordingly to control the welding process in a bid to achieve the desired penetration state. Because of their sensory capabilities and experience-based behavior, they are sometimes more preferred than automated welding machines. However, physical limitations of the human welder including inattention, fatigue, stress and long-term health issues, etc, do not exist in automated welding machines [8]. The mechanism of human welder's experience-based behavior thus should be fully explored. The resultant welder behavior models may also help resolve the skilled welder shortage.

The associate editor coordinating the review of this manuscript and approving it for publication was Inês Domingues .

The core of the automated welding system [9]–[11] is the control algorithm, which processes the information collected by the sensor, extracts the feature information of the weld, and obtains the deviation signal through a certain algorithm. Welding processing methods generally contain quantification, information processing [12]–[14], image recognition [15]–[17] and other steps to obtain the precise position and track of weld position. It is a vital problem, which needs to be solved by the control method, to figure out how to use the information to control the actuators to track and obtain stable and ideal welding quality during the welding process. With the continuous progress in science and technology, especially the rapid advancement of computer technology, control technology has also been rapidly developed. The control methods that have been widely applied and will be applied in modern welding production are as follows: Huang *et al.* [18] proposed a neural network algorithm for weld detection based on adaptive resonance theory. The neural network was applied to automatically identify weld types, which was rapid, stable and highly reliable, and was an ideal method for automatic identification of weld types. Zhu *et al.* [15] proposed a two-stage template matching method to identify the starting point of the weld. Firstly, the global matching

method was used to eliminate the obvious wrong data points, and then the local dynamic search method was used to find the starting point of the weld. However, this method only identifies the starting point of the weld in the image space, and does not realize the positioning control of the welding gun moving to the starting point of the weld. By identifying this active target, Zhang *et al.* [19] indirectly identified the initial position of the weld seam. This method has good robustness, but the final identification accuracy depends on the manual placement position of the active target, and the additional operation of placing the active target which also restricts its usage in narrow or unknown space. Zhang *et al.* [20] used a novel 3d vision sensing system to measure the characteristic parameters of tungsten arc welding pool in real time. The linear welding model is improved by introducing the nonlinear operating point, and the developed control system can effectively realize the welding depth requirement of the welded joint under various disturbance conditions. Liu *et al.* [21] used a novel machine vision system to measure the surface of mirror pool in real time. The full-penetration welds with different weld widths were obtained by experiments under different welding conditions, and the corresponding images were obtained, which were used for the reconstruction of weld pool surface and the calculation of optimal model characteristic parameters. Liu *et al.* [22] constructed an adaptive neural fuzzy reasoning system (ANFIS) and implemented it as an intelligent controller in the automatic GTAW process. The robustness of the controller was verified by closed-loop control experiments.

In real automated welding system, there are many constraints, such as the external disturbances, model uncertainties and a large amount of calculation, which are not in accordance with the assumption of control algorithm and bring difficulties to its application. Thus, the author aims to design a new control algorithm to perfect exact tip tracking in this article. The introduction of ILC [23]–[25], which has the characteristics of strong anti-interference, low cost and high speed, meets these requirements. ILC does not depend on the precise model of the controlled system instead of using the previous control information to build the current control signal. Liu *et al.* [26] proposed a data-driven artificial intelligence modeling method and used it to control the automatic tungsten gas arc welding process. In order to further improve the calculation accuracy, the iterative control method is adopted, and the iterative local ANFIS model has a better modeling performance, revealing the more detailed intelligence of welders. However, due to the data dropout and external disturbance, the direct application of traditional open-closed-loop ILC [27], [28] to GTAW may lead to a poor performance. In iterative learning control, open-closed-loop learning law is actually a kind of feed-forward and feedback control. It is likely to have a large control error even when it meets the convergence condition. So we introduce a self-adjustive factor, which can reduce the system error, improve the system's stability, and speeds up the learning speed. In this work, Open-closed-loop iterative learning

control with a self-adjustive factor law is chosen as the controller for GTAW process.

This article is organized as follows, In Section 2, dynamics model of the GTAW system is presented. Section 3 describes the control strategy. The convergence analysis of the proposed algorithm is presented in Section 4. Section 5 describes the numerical simulation analysis, and finally Section 6 is the conclusion.

## II. DYNAMIC MODEL OF GTAW SYSTEM

The process of GTAW (gas tungsten arc welding) is shown in Figure 1: clamping the tungsten electrode to electrode holder, stretching it out through the tip of the welding torch and then using the arc produced between tungsten electrode and base material to weld materials. When the procedure begins, arc conducts heat to the base material and temperature rises rapidly. Then, partial weld area will be melted into a weld pool. If you need to add metals to the weld pool, please add from the front tip of the arc at a certain speed.

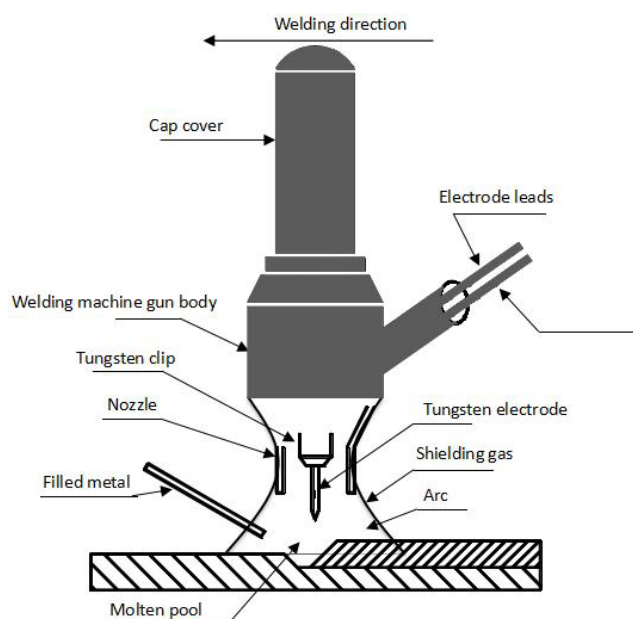


FIGURE 1. Schematic diagram of GTAW welding process.

During the procedure of GTAW, the most important standard of high-quality welding is to make sure that the material is fully melted. The most direct and effective measure of melting level is back-bead width of molten pool. Therefore, the control of molten degree can be boiled down to the control of back-bead width. During the formation of welding seam, the welding current is a critical parameter. From the perspective of system control, back-bead width of molten pool can be controlled as uniform as possible by adjusting the welding current. In this research of the welding process of GTAW, we set welding current as control input and the back-bead width as output of the system.

The dynamic characteristic model of GTAW welding system is as follows:

$$x(t) = \sum_{l=1}^j a_l x(t-l) + \sum_{h=1}^k b_h u(t-h) \quad (1)$$

where  $x(t)$  is the back weld width,  $u(t)$  is the welding current,  $l$  and  $h$  are the system time delay,  $j = 5, k = 6$ .

Formula (1) can be written as:

$$\begin{aligned} X(t) &= \begin{bmatrix} x(t) \\ x(t-1) \\ x(t-2) \\ x(t-3) \\ x(t-4) \end{bmatrix} \\ &= \begin{bmatrix} a1 & a2 & a3 & a4 & a5 \\ 1 & 0 & 0 & 0 & 0 \\ 0 & 1 & 0 & 0 & 0 \\ 0 & 0 & 1 & 0 & 0 \\ 0 & 0 & 0 & 1 & 0 \end{bmatrix} \begin{bmatrix} x(t-1) \\ x(t-2) \\ x(t-3) \\ x(t-4) \\ x(t-5) \end{bmatrix} \\ &+ \begin{bmatrix} b1 & b2 & b3 & b4 & b5 & b6 \\ 0 & 0 & 0 & 0 & 0 & 0 \\ 0 & 0 & 0 & 0 & 0 & 0 \\ 0 & 0 & 0 & 0 & 0 & 0 \\ 0 & 0 & 0 & 0 & 0 & 0 \\ 0 & 0 & 0 & 0 & 0 & 0 \end{bmatrix} \begin{bmatrix} u(t-1) \\ u(t-2) \\ u(t-3) \\ u(t-4) \\ u(t-5) \\ u(t-6) \end{bmatrix} \quad (2) \end{aligned}$$

The equation of state of model (1) is expressed as:

$$\begin{cases} X(t) = AX(t-1) + BU(t) \\ Y(t) = CX(t) \end{cases} \quad (3)$$

where  $A = \begin{bmatrix} a1 & a2 & a3 & a4 & a5 \\ 1 & 0 & 0 & 0 & 0 \\ 0 & 1 & 0 & 0 & 0 \\ 0 & 0 & 1 & 0 & 0 \\ 0 & 0 & 0 & 1 & 0 \end{bmatrix}, B = \begin{bmatrix} b1 & b2 & b3 & b4 & b5 & b6 \\ 0 & 0 & 0 & 0 & 0 & 0 \\ 0 & 0 & 0 & 0 & 0 & 0 \\ 0 & 0 & 0 & 0 & 0 & 0 \\ 0 & 0 & 0 & 0 & 0 & 0 \\ 0 & 0 & 0 & 0 & 0 & 0 \end{bmatrix},$   
 $C = I.$

### III. DESIGNED CONTROLLER AND SELF-ADJUSTIVE FACTOR

To do this, we use following open-closed-loop P-type ILC scheme:

$$\begin{aligned} u_{i+1}(t) &= \Upsilon(i, t) u_0(t) + (1 - \Upsilon(i, t)) u_i(t) \\ &+ \varphi(t) e_i(t) + \Psi(t) e_{i+1}(t) \end{aligned} \quad (4)$$

where  $i$  indicates the iteration number;  $\varphi(t)$  is the open-loop proportional learning gain matrix;  $\Psi(t)$  is the closed-loop proportional learning gain matrix;  $u_i(t)$  is the control variable;  $u_0(t)$  is the initial value of the input; and  $e_i(t) = y_d(t) - y_i(t)$ .

This multivariable self-adjustive factor  $\Upsilon(i, t)$  can vary automatically according to changing system deviation and derivative of error. The factor  $\Upsilon(i, t)$  is used to balance perfect learning and robustness, which can increase the

robustness of ILC against uncertainty, disturbance, initialization error, and fluctuation of system dynamics:

$$\Upsilon(i, t) = (1 - \mu) / 30^{\max[\kappa e_i^2(t) + 0.1 * \dot{\kappa} e_i^2(t)]} \quad (5)$$

where  $\kappa$  coordinates gain changes and  $\mu$  is used to control the rate at which  $\mu$  approaches 1.

### IV. CONVERGENCE ANALYSIS

Due to repeatability, interference and uncertainty in the welding process, the welding process is repeated at  $[0, T]$ . Formula (3) can be written as:

$$\begin{cases} X_i(t) = AX_i(t-1) + BU_i(t) + \omega_i(t) \\ Y_i(t) = CX_i(t) + v_i(t) \end{cases} \quad (6)$$

where  $i$  is the number of iterations,  $t \in \{0, 1, \dots, T\}$ .  $\omega_i(t)$  and  $v_i(t)$  are the uncertainty item and interferential term, respectively.

To get a convergence condition, we assume the following restrictions on the GTAW system:

*Assumption 1:* The initial state of the system is the same every time;

*Assumption 2:* The expected output is the same, when the system runs every time;

*Assumption 3:* There exist  $u_d(t)$  that makes system state become  $x_d(t)$  and system output become  $y_d(t)$  for all  $t \in [0, T]$ .

$$\begin{cases} x_d(t) = Ax_d(t-1) + Bu_d(t) + \omega_d(t) \\ y_d(t) = Cx_d(t) \end{cases} \quad (7)$$

where  $x_d(t)$  is the expected state. In the actual welding process, the welding control system performing the repeated welding process meets the above three assumptions. For batch welding of the same workpiece, the starting point of each welding process is the same, thus meeting **Assumption 1**. The expected output in the welding process is constant value, so it also meets **Assumption 2**. **Assumption 3** is the condition of controllability for a given control task.

When the initial state of the system is  $x_i(0)$ , the solution of equation (6) can be written as:

$$x_i(t) = A^t x_i(0) + \sum_{s=0}^t A^{t-s} B u_i(s), t \in \{0, T\} \quad (8)$$

*Lemma:* For the system described by equation (6), the given reachable expected trajectory is  $y_d(t)$ , If the condition (1) and (2),

$$(1) \quad \left\| \frac{(1 - \Upsilon) - \varphi CB}{I + \Psi CB} \right\| \leq \rho < 1, t \in \{0, T\}$$

$$(2) \quad x_i(0) = x_d(0), \quad i = 0, 1, 2, \dots$$

Then, the learning rate (4) makes the output trajectory uniformly converge to the expected trajectory. When  $i \rightarrow \infty$ ,  $y_i(t) \rightarrow y_d(t) (t \in [0, T + 1])$ .

The control error of the  $i + 1$  iteration is investigated,

$$\begin{aligned} \Delta u_{i+1}(t) &= u_d(t) - u_{i+1}(t) = u_d(t) - \Upsilon u_0(t) \\ &\quad - (1 - \Upsilon) u_i(t) - \varphi e_i(t) - \Psi e_{i+1}(t) \\ &= \Upsilon \Delta u_0(t) + (1 - \Upsilon) \Delta u_i(t) \\ &\quad - \varphi [y_d(t) - y_i(t)] - \Psi [y_d(t) - y_{i+1}(t)] \\ &= \Upsilon \Delta u_0(t) + (1 - \Upsilon) \Delta u_i(t) - \varphi C \Delta x_i(t) \\ &\quad - \Psi C \Delta x_{i+1}(t) + \varphi C v_i(t) + \Psi C v_{i+1}(t) \\ &= \Upsilon \Delta u_0(t) + (1 - \Upsilon) \Delta u_i(t) \\ &\quad - \varphi C [A \Delta x_i(t-1) + B \Delta u_i(t) + \Delta \omega_i(t)] \\ &\quad - \Psi C [A \Delta x_{i+1}(t-1) + B \Delta u_{i+1}(t) + \Delta \omega_{i+1}(t)] \\ &\quad + \varphi C v_i(t) + \Psi C v_{i+1}(t) \end{aligned} \tag{9}$$

From (9) can be obtained

$$\begin{aligned} (I + \Psi C B) \Delta u_{i+1}(t) &= ((1 - \Upsilon) - \varphi C B) \Delta u_i(t) \\ &\quad - \varphi C A \Delta x_i(t-1) - \Psi C A \Delta x_{i+1}(t-1) \\ &\quad + \varphi C (v_i(t) - \Delta \omega_i(t)) + \Upsilon \Delta u_0(t) \\ &\quad + \Psi C (v_{i+1}(t) - \Delta \omega_{i+1}(t)) \end{aligned} \tag{10}$$

Take the norm at both ends of formula (10):

$$\begin{aligned} \|I + \Psi C B\| \|\Delta u_{i+1}(t)\| &= \|(1 - \Upsilon) - \varphi C B\| \|\Delta u_i(t)\| \\ &\quad + \|\varphi C A\| \|\Delta x_i(t-1)\| + \|\Upsilon \Delta u_0(t)\| \\ &\quad + \|\Psi C A\| \|\Delta x_{i+1}(t-1)\| \\ &\quad + \|\varphi C\| \|v_i(t) - \Delta \omega_i(t)\| \\ &\quad + \|\Psi C\| \|v_{i+1}(t) - \Delta \omega_{i+1}(t)\| \end{aligned} \tag{11}$$

According to formula (11), we obtain

$$\begin{aligned} \|\Delta u_{i+1}(t)\| &\leq \left\| \frac{(1 - \Upsilon) - \varphi C B}{I + \Psi C B} \right\| \|\Delta u_i(t)\| \\ &\quad + \left\| \frac{\varphi C A}{I + \Psi C B} \right\| \|\Delta x_i(t-1)\| \\ &\quad + \left\| \frac{\Psi C A}{I + \Psi C B} \right\| \|\Delta x_{i+1}(t-1)\| \\ &\quad + \left\| \frac{\varphi C + \Psi C}{I + \Psi C B} \right\| (\zeta_v - \zeta_\omega) \\ &\quad + \left\| \frac{\Upsilon}{I + \Psi C B} \right\| \|\Delta u_0(t)\| \\ &\leq \rho \|\Delta u_i(t)\| + \eta_1 \|\Delta x_i(t-1)\| \\ &\quad + \eta_3 \|\Delta x_{i+1}(t-1)\| + \Theta \end{aligned} \tag{12}$$

where  $\eta_1 = \|\frac{\varphi C A}{I + \Psi C B}\|$ ,  $\eta_3 = \|\frac{\Psi C A}{I + \Psi C B}\|$ ,  $\zeta_\omega = \max\{\sup_{t \in [0, T]} \|\Delta \omega_i(t)\|, \sup_{t \in [0, T]} \|\Delta \omega_{i+1}(t)\|\}$ ,  $\Theta = \|\frac{\varphi C + \Psi C}{I + \Psi C B}\|(\zeta_v - \zeta_\omega) + \|\frac{\Upsilon}{I + \Psi C B}\| \|\Delta u_0(t)\|$ ,  $\zeta_v = \max_{t \in [0, T]} \{\sup \|v_i(t)\|, \sup \|v_{i+1}(t)\|\}$ ,  $\rho = \|\frac{(1 - \Upsilon) - \varphi C B}{I + \Psi C B}\|$ .

Using formula (8), formula (11) can be written as:

$$\begin{aligned} \|\Delta u_{i+1}(t)\| &\leq \rho \|\Delta u_i(t)\| + \eta_1 \sum_{s=0}^{t-1} \|A^{t-s} B\| \|\Delta u_i(s)\| \\ &\quad + \eta_3 \sum_{s=0}^{t-1} \|A^{t-s} B\| \|\Delta u_{i+1}(s)\| + \Theta \\ &\leq \rho \|\Delta u_i(t)\| + \eta_1 \eta_2 \sum_{s=0}^{t-1} \|\Delta u_i(s)\| \\ &\quad + \eta_3 \eta_2 \sum_{s=0}^{t-1} \|\Delta u_{i+1}(s)\| + \Theta \end{aligned} \tag{13}$$

where  $1 \leq t \leq T$ ,  $\eta_2 = \sup_{0 \leq s \leq t-1} \|A^{t-s} B\|$ .

Multiply both sides of formula (13) by  $\lambda^t$  ( $0 < \lambda < 1$ ), we obtain

$$\begin{aligned} \lambda^t \|\Delta u_{i+1}(t)\| &\leq \rho \lambda^t \|\Delta u_i(t)\| + \eta_1 \eta_2 \sum_{s=0}^{t-1} \lambda^{t-s} \lambda^s \|\Delta u_i(s)\| \\ &\quad + \eta_3 \eta_2 \sum_{s=0}^{t-1} \lambda^{t-s} \lambda^s \|\Delta u_{i+1}(s)\| + \Theta \\ &\leq \rho \lambda^t \|\Delta u_i(t)\| + \Theta \\ &\quad + \eta_1 \eta_2 \sum_{s=0}^{t-1} \lambda^{t-s} \sup_{0 \leq \tau \leq T} \{\lambda^\tau \|\Delta u_i(\tau)\|\} \\ &\quad + \eta_3 \eta_2 \sum_{s=0}^{t-1} \lambda^{t-s} \sup_{0 \leq \tau \leq T} \{\lambda^\tau \|\Delta u_{i+1}(\tau)\|\} \\ &\leq \rho \lambda^t \|\Delta u_i(t)\| + \eta_1 \eta_2 \sum_{s=0}^{t-1} \lambda^{t-s} \|\Delta u_i\|_\lambda \\ &\quad + \eta_3 \eta_2 \sum_{s=0}^{t-1} \lambda^{t-s} \|\Delta u_{i+1}\|_\lambda + \Theta \\ &\leq \rho \lambda^t \|\Delta u_i(t)\| + \eta_1 \eta_2 \frac{\lambda(1 - \lambda^T)}{1 - \lambda} \|\Delta u_i\|_\lambda \\ &\quad + \eta_3 \eta_2 \frac{\lambda(1 - \lambda^T)}{1 - \lambda} \|\Delta u_{i+1}\|_\lambda + \Theta \end{aligned} \tag{14}$$

According to formula (11) and the definition of norm, we get

$$\|\Delta u_{i+1}\|_\lambda \leq \tilde{\rho} \|\Delta u_i\|_\lambda + \Theta \tag{15}$$

where  $\tilde{\rho} = \frac{\rho(1-\lambda) + \eta_1 \eta_2 \lambda(1-\lambda^T)}{1 - \lambda - \eta_3 \eta_2 \lambda(1-\lambda^T)}$ .

When  $\rho < 1$ , we can get  $\lim_{i \rightarrow \infty} \|\Delta u_i\|_\lambda \leq \frac{\Theta}{1 - \tilde{\rho}}$ . According to formula (6) and (8), when  $0 < \lambda < 1$ , we get

$$\begin{aligned} \lambda^t \|e_i(t)\| &\leq \|C\| \sum_{s=0}^{t-1} \|A^{t-s} B\| \lambda^{t-s} \lambda^s \|\Delta u_i(s)\| \\ &\leq \hat{c} \eta_2 \sum_{s=0}^{t-1} \lambda^{t-s} \|\Delta u_i\|_\lambda \\ &\leq \hat{c} \eta_2 \frac{\lambda(1 - \lambda^T)}{1 - \lambda} \|\Delta u_i\|_\lambda \end{aligned} \tag{16}$$

where  $1 \leq t \leq T + 1$ ,  $\hat{c} = \|C\|$ .

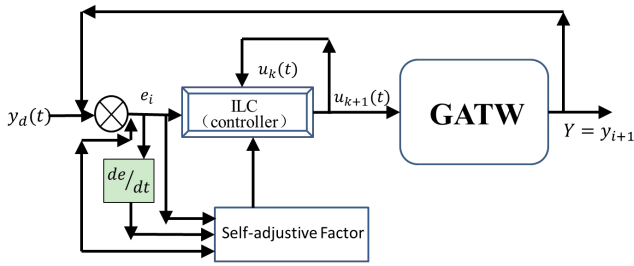


FIGURE 2. A block diagram of the designed ILC law.

According to the definition of  $\lambda$ -norm:

$$\sup_{1 \leq t \leq T+1} \{\lambda^t \|e_i(t)\|\} \leq \hat{c}\eta_2 \frac{\lambda(1-\lambda^T)}{1-\lambda} \|\Delta u_i\|_\lambda \quad (17)$$

So  $\lim_{i \rightarrow \infty} \sup_{0 \leq t \leq T} \{\lambda^t \|e_i(t)\|\} \leq \frac{\Theta}{1-\rho}$ . We find that the tracking error bound converges to a small neighborhood of the origin, we can reach the conclusion  $y_i(t) \rightarrow y_d(t) (i \rightarrow \infty)$ .

V. SIMULATION AND ANALYZE

In this section, the proposed algorithm is applied to the automatic welding system. Let set the input initial value  $u_i(t) = 0$  at each iteration. The expected width of the back of the pool is  $y_d(t) = 5\text{mm}$ . The data used in the simulation are  $\varphi(t) = 0.2$ ,  $\psi(t) = 0.15$ ,  $\kappa = 4$ ,  $\omega_i(t) = 0.001 \sin(0.1\pi t)$  and  $\mu = 0.65$ .

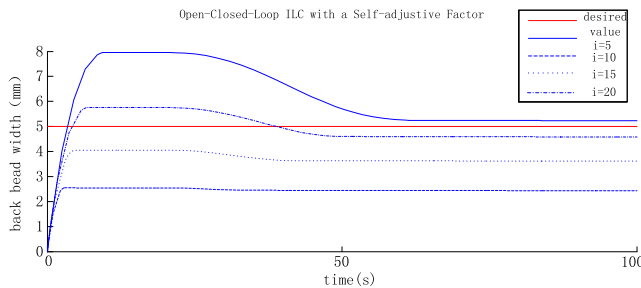


FIGURE 3. Back melt width tracking curve of the designed ILC law.

During the welding process, the tracking process of the iterative learning control algorithm are shown in Figure 3 and Figure 4. Figure 5 and Figure 6 show the maximum tracking errors from iteration to iteration controlled by ILC. The open-closed-loop ILC with a self-adjustive factor obtained very good tracking performance with very small tracking errors in the direction even under the non-repetitive disturbance conditions. It is shown that the traditional open-closed-loop ILC obtain acceptable tracking performance, while the ILC with a self-adjustive factor still performs much better than the open-closed-loop ILC. The proposed ILC algorithm converges to approximate small zero errors at the 8rd iteration while open-closed-loop ILC still has small bounded tracking errors. And it has a faster rate of convergence. These results fully illustrate the importance of the self-adjustive factor. It demonstrates again that the proposed ILC algorithm can

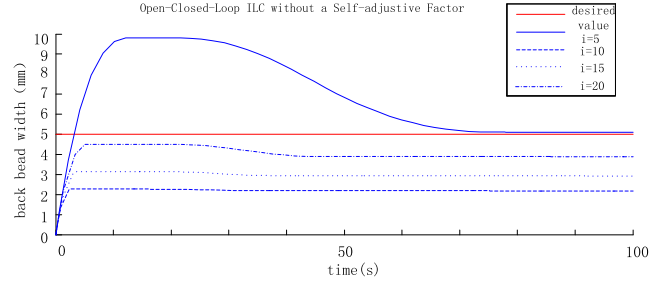


FIGURE 4. Back melt width tracking curve of the traditional ILC law.

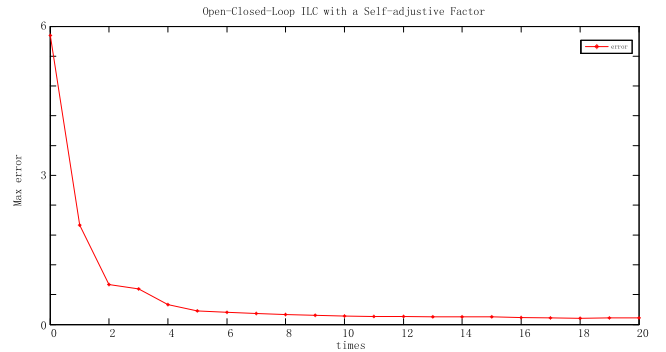


FIGURE 5. Maximum tracking error in iteration times with self-adjustive factor.

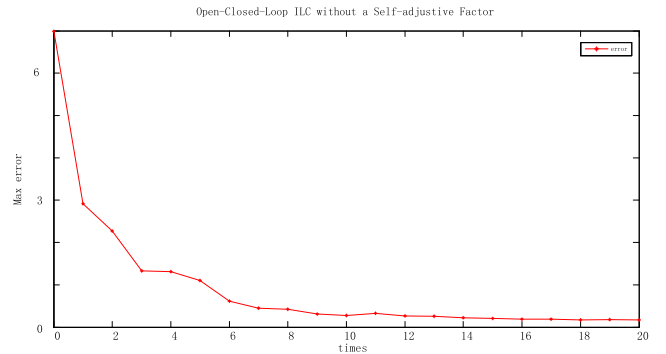


FIGURE 6. Maximum tracking error in iteration times without self-adjustive factor.

obtain much better tracking performances even under the existence of disturbances and uncertainties.

Also, the iterative learning controller shows better convergence results through iteration control. The algorithm is simple, and it can realize the actual motion track in the given time horizon. Simulation results show that the proposed algorithm is effective in controlling both the welding precision and in achieving full best effect even under the condition of external interference.

VI. CONCLUSION

In this article, an innovative ILC approach to control the welding process is proposed. The proposed algorithm can realize the complete automation of welding process through intelligent control, guarantee welding quality and improve



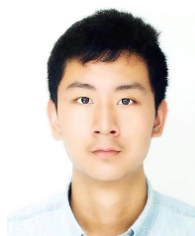
welding production efficiency. Automated control simulations are conducted and results verified the effectiveness of the proposed controller under welding speed disturbance. With the continuous development of computer control technology, the advancement of automatic welding control technology and the intelligent welding which can accurately track and adjust the welding track in real time have become an important development trend in the field of welding.

## REFERENCES

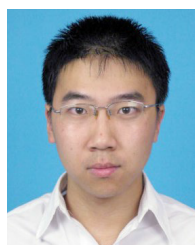
- [1] K. R. Ramkumar and S. Natarajan, "Optimization of GTAW al 3003 weld using fabricated nanocomposite filler metal," *Mater. Manuf. Process.*, vol. 34, no. 3, pp. 293–302, Feb. 2019.
- [2] A. Pai, I. Sogalad, S. Basavarajappa, and P. Kumar, "Results of tensile, hardness and bend tests of modified 9Cr 1Mo steel welds: Comparison between cold wire and hot wire gas tungsten arc welding (GTAW) processes," *Int. J. Pressure Vessels Piping*, vol. 169, pp. 125–141, Jan. 2019.
- [3] S. Chen, G. Guillemot, and C.-A. Gandin, "3D coupled cellular automaton (CA)-finite element (FE) modeling for solidification grain structures in gas tungsten arc welding (GTAW)," *ISIJ Int.*, vol. 54, no. 2, pp. 401–407, 2014.
- [4] N. Lv, J. Zhong, J. Wang, and S. Chen, "Automatic measuring and processing system of audio sensing for real-time arc height control of pulsed GTAW," *Sensor Rev.*, vol. 34, no. 1, pp. 51–66, Jan. 2014.
- [5] Y. Su, W. Li, X. Wang, T. Ma, L. Ma, and X. Dou, "The sensitivity analysis of microstructure and mechanical properties to welding parameters for linear friction welded rail steel joints," *Mater. Sci. Eng., A*, vol. 764, Sep. 2019, Art. no. 138251.
- [6] R. Nandhini, R. D. Kumar, S. Muthukumar, and S. Kumaran, "Optimization of welding process parameters in novel friction stir welding of polyamide 66 joints," *Mater. Sci. Forum*, vol. 969, pp. 828–833, Aug. 2019.
- [7] P. Shreyas, B. Panda, and R. Kumar, "Effect of various welding parameters on the mechanical behaviour of 316L stainless steel-galvanized steel weld," *Mater. Sci. Forum*, vol. 969, pp. 807–812, Aug. 2019.
- [8] M. Čačo, R. Kohár, S. Hřeček, R. Tribula, and P. Ščerba, "Use the method of TRIZ in optimizing automated machine for ultrasonic welding," *Procedia Eng.*, vol. 192, pp. 80–85, Jan. 2017.
- [9] P. Kiddee, Z. Fang, and M. Tan, "An automated weld seam tracking system for thick plate using cross mark structured light," *Int. J. Adv. Manuf. Technol.*, vol. 87, nos. 9–12, pp. 3589–3603, Dec. 2016.
- [10] E. A. Kuper, P. V. Logachev, V. V. Repkov, A. N. Selivanov, P. A. Selivanov, Y. I. Semenov, A. G. Tribendis, M. G. Fedotov, and A. S. Chertovskikh, "Automated system for setting the seam coordinates in electron-beam welding facilities," *Optoelectron., Instrum. Data Process.*, vol. 51, no. 1, pp. 45–50, Jan. 2015.
- [11] A. Caggiano, L. Nele, E. Sarno, and R. Teti, "3D digital reconfiguration of an automated welding system for a railway manufacturing application," *Procedia CIRP*, vol. 25, pp. 39–45, Jan. 2014.
- [12] D. A. Sanders, G. Lambert, J. Graham-Jones, G. E. Tewkesbury, S. Onuh, D. Ndzi, and C. Ross, "A robotic welding system using image processing techniques and a CAD model to provide information to a multi-intelligent decision module," *Assem. Autom.*, vol. 30, no. 4, pp. 323–332, Sep. 2010.
- [13] T. Morita, Y. Ogawa, and T. Sumitomo, "331 development of image processing technology to construct welding technology information database," in *Proc. Mater. Process. Conf.*, vol. 9, 2001, pp. 353–354.
- [14] H. Wang, Y. Zhang, and G. Chen, "Resistance spot welding processing monitoring based on electrode displacement curve using moving range chart," *Meas.*, vol. 42, no. 7, pp. 1032–1038, 2009.
- [15] Z. Y. Zhu, T. Lin, Y. J. Piao, and S. B. Chen, "Recognition of the initial position of weld based on the image pattern match technology for welding robot," *Int. J. Adv. Manuf. Technol.*, vol. 26, nos. 7–8, pp. 784–788, Oct. 2005.
- [16] X. Wang, "Recognition of welding defects in radiographic images by using support vector machine classifier," *Res. J. Appl. Sci., Eng. Technol.*, vol. 2, no. 3, pp. 295–330, 2010.
- [17] X. Gao, D. You, and S. Katayama, "Infrared image recognition for seam tracking monitoring during fiber laser welding," *Mechatronics*, vol. 22, no. 4, pp. 370–380, Jun. 2012.
- [18] S. Huang, Y. Qian, S. Huang, and Y. Qian, "Welding seam detecting algorithm based on the art artificial neural network," *Chin. J. Mech. Eng.*, vol. 93, no. 2, pp. 175–194, 1994.
- [19] J. Q. Zhang and H. Zhang, "Recognition and locating of object based on image-processing for mobile robot," *Comput. Meas. Control*, vol. 14, no. 5, pp. 673–675, 2006.
- [20] B. W. Zhang, Y. Liu, and X. Wang, "Characterization of three dimensional weld pool surface in GTAW," *Weld. J.*, vol. 91, no. 7, pp. 195S–203S, 2012.
- [21] Y. K. Liu and Y. M. Zhang, "Model-based predictive control of weld penetration in gas tungsten arc welding," *IEEE Trans. Control Syst. Technol.*, vol. 22, no. 3, pp. 955–966, May 2014.
- [22] Y. Liu, W. Zhang, and Y. Zhang, "Dynamic neuro-fuzzy-based human intelligence modeling and control in GTAW," *IEEE Trans. Autom. Sci. Eng.*, vol. 12, no. 1, pp. 324–335, Jan. 2015.
- [23] S. Liu, J. Wang, D. Shen, and D. O'Regan, "Iterative learning control for noninstantaneous impulsive fractional-order systems with varying trial lengths," *Int. J. Robust Nonlinear Control*, vol. 28, no. 18, pp. 6202–6238, Dec. 2018.
- [24] X. Wang, J. Wang, D. Shen, and Y. Zhou, "Convergence analysis for iterative learning control of conformable fractional differential equations," *Math. Methods Appl. Sci.*, vol. 41, no. 17, pp. 8315–8328, Nov. 2018.
- [25] X. Deng, X. Sun, R. Liu, and S. Liu, "Consensus control of leader-following nonlinear multi-agent systems with distributed adaptive iterative learning control," *Int. J. Syst. Sci.*, vol. 49, no. 16, pp. 3247–3260, Dec. 2018.
- [26] Y. Liu and Y. Zhang, "Iterative local ANFIS-based human welder intelligence modeling and control in pipe GTAW process: A data-driven approach," *IEEE/ASME Trans. Mechatronics*, vol. 20, no. 3, pp. 1079–1088, Jun. 2015.
- [27] X. Y. Cheng, H. B. Wang, Y. L. Jia, and Y. Dong, "Open-closed-loop iterative learning control for a class of nonlinear systems with random data dropouts," *IOP Conf. Ser., Mater. Sci. Eng.*, vol. 359, May 2018, Art. no. 012009.
- [28] S.-K. Wang, J.-B. Zhao, and J.-Z. Wang, "Open-closed-loop iterative learning control for hydraulically driven fatigue test machine of insulators," *J. Vib. Control*, vol. 21, no. 12, pp. 2291–2305, Sep. 2015.



**NAN YIN** received the Ph.D. degree in management science from Dhurakij Pundit University, Thailand. He is currently a Lecturer with the Business School, Nanjing Xiaozhuang University, China. His research interests include management information systems and data mining, as well as the relevant work experience of enterprise network construction and data analysis, with strong practical work experience.



**LIU HANWEN** is currently pursuing the bachelor's degree with the Department of Transportation Engineering, Tongji University, majoring in traffic and transportation. He has participated as the youngest member in the 2018 Tongji Departmental Project "Shanghai Metro System's Security Screening," which won the First Place in the Department of Transportation Engineering.



**YANG WU** was born in 1986. He received the B.S. degree in automation from Zhejiang University, China, in 2009. He is currently a Lecturer with Wuxi Taihu University. His research interests include pattern recognition, machine vision, and deep learning.

...